International Journal of Advanced Multidisciplinary Research and Studies

Chitosan Nanoparticles Encapsulating *Ipomoea digitata* L. Tuber and *Jatropha gossypiifolia* L. leaf Extract Suppress NF-κB, Wnt/β-catenin, and MAPK Signaling Pathways in HCT116 and SW480 Colorectal Cancer Cells

[1] **Cletus Anes Ukwubile,** [2] **Aliyu Nuhu,** [3] **Ademola Clement Famurewa,** [4] **Henry Nettey,** [5] **Jude Amakaeze Odugu**
[1] Department of Pharmacognosy, Faculty of Pharmacy, University of Maiduguri, Maiduguri, Nigeria
[2] Department of Pharmacognosy and Ethnopharmacy, Faculty of Pharmacy, University of Abuja, Nigeria
[3] Department of Medical Biochemistry, Alex Ekwueme Federal University, Ndufu Alike, Ikwo, Nigeria
[4] Department of Pharmaceutics and Microbiology, School of Pharmacy, University of Ghana, Legon, Ghana
[5] Department of Medical Microbiology, Federal Medical Centre Kubwa Abja, Nigeria

Corresponding Author: **Cletus Anes Ukwubile**

Abstract

Ipomoea digitata and *Jatropha gossypiifolia* are traditional medicinal plants that have been widely used in indigenous medicine for their anti-inflammatory and anticancer benefits. Despite their long-standing use, scientific understanding of how effective they are against colorectal cancer and how they might influence the cancer-related signaling pathways remains limited and requires further research. The study was aimed at evaluating the anticancer and anti-inflammatory properties of *I. digitata* tuber and *J. gossypiifolia* leaf extracts encapsulated in chitosan nanoparticles (CSNPs), particularly examining their effects on inhibiting NF-κB, Wnt/β-catenin, and MAPK signaling pathways in colorectal cancer models. Methanol extracts from the tubers of *I. digitata* and the leaves of *J. gossypiifolia* were encapsulated into chitosan nanoparticles through the ionic gelation method. The physicochemical characteristics of these chitosan nanoparticles, including particle size, zeta potential, and encapsulation efficiency, were analyzed using dynamic light scattering (DLS) and transmission electron microscopy (TEM). Their cytotoxic effects were evaluated against HCT116 and SW480 colorectal cancer cell lines using the MTT assay. Apoptosis induction was confirmed by observing increased caspase-3 activity and through fluorescence microscopy with an Annexin V/PI apoptosis detection kit. The expression of key oncogenic signaling molecules- NF-κB p65, β-catenin, ERK1/2, and p38 MAPK were examined by Western blotting and quantitative PCR. Additionally, anti-inflammatory effects were assessed by measuring levels of TNF-α, IL-6, and COX-2 using enzyme-linked immunosorbent assay (ELISA). The chitosan nanoparticles (CSNPs) exhibited a uniform size distribution with an average particle size of approximately 180 nm, and the encapsulation efficiency of the plant extracts was high (>85%). The nanoparticles demonstrated controlled release profiles over 48 hours. Treatment with extract-loaded CSNPs resulted in a significant reduction in cell viability in both HCT116 and SW480 colorectal cancer cells, with IC_{50} values of 22.3 ± 2.1 μg/mL and 34.8 ± 3.4 μg/mL, respectively, compared to free extracts (IC_{50} values: 40.5 ± 4.3 μg/mL for HCT116 and 52.1 ± 3.9 μg/mL for SW480). Apoptotic cell death was confirmed by increased caspase-3 activity, with a 2.3-fold increase in both cell lines following treatment with the extract-loaded CSNPs (p < 0.05). Fluorescence microscopy analysis of Annexin V/PI-stained cells revealed a significant increase in early and late apoptotic cells, with 43.5% and 35.6% of HCT116 and SW480 cells, respectively, exhibiting apoptosis after treatment, compared to 18.2% and 14.7% in the untreated control groups. Molecular analysis further revealed significant downregulation of key oncogenic proteins, including NF-κB p65, β-catenin, and ERK1/2. Additionally, the extract-loaded CSNPs significantly reduced the expression of pro-inflammatory cytokines such as TNF-α (by 45.3 ± 4.2%), IL-6 (by 48.7 ± 5.1%), and COX-2 (by 50.2 ± 3.8%) in treated cells. Chitosan nanoparticles carrying extracts from *I. digitata* and *J. gossypiifolia* have been shown to effectively slow down the growth of colorectal cancer cells by targeting important cancer-related and inflammatory pathways. This study not only validates the ethnomedicinal uses of these plants but also highlights their potential as promising natural options for developing new treatments against colorectal cancer.

1. Introduction

Colorectal cancer (CRC) is one of the most common and deadly cancers worldwide, ranking third in how often it occurs and second in the number of deaths it causes (Sung *et al*., 2021) [30]. While treatments like chemotherapy, targeted therapies, and surgery have improved over the years, the outlook for people with advanced CRC remains challenging. This is mainly because

cancer often becomes resistant to treatment, spreads to other parts of the body, and frequently comes back. Research shows that ongoing inflammation and disruptions in key cellular signaling pathways—such as NF-κB, Wnt/β-catenin, and MAPK play a major role in the development and progression of colorectal cancer(Fearon *et al*., 2011; Grivennikov *et al*., 2010) [7, 10]. These pathways not only encourage cancer cells to grow uncontrollably but also help them evade programmed cell death and create an inflammatory environment that supports tumor growth. This highlights the urgent need for new treatments that can target and regulate these underlying processes more effectively.

Natural products and plant-based compounds have long been a valuable source of cancer-fighting drugs, with well-known examples like paclitaxel and camptothecin coming directly from medicinal plants(Malviya *et al*., 2023) [22]. Traditional knowledge about how different cultures use plants for healing, especially for conditions like inflammation, tumors, and infections provides a treasure trove of potential new compounds that could target multiple pathways involved in colorectal cancer. However, despite their promise, many of these plant-derived substances face challenges such as poor solubility, low absorption in the body, and quick breakdown, which make it difficult to develop them into effective treatments for patients.

Nanotechnology-based drug delivery systems, particularly those using chitosan nanoparticles (CSNPs), hold great promise in addressing these challenges. Chitosan is a natural substance that's biodegradable, compatible with the body, and can stick to mucous membranes, making it an excellent carrier for plant-based compounds (J. Li *et al*., 2018) [17]. By encapsulating these natural compounds within CSNPs, we can greatly improve their stability and solubility and deliver them more precisely to the target sites in the body. This approach not only enhances how well the compounds are absorbed and used by cells but also boosts their effectiveness in fighting disease while reducing harmful side effects throughout the body.

Ipomoea digitata L., commonly known as "Ji-nnu" in the Igbo tribe in Nigeria and belonging to the *Convolvulaceae* family, is a well-regarded medicinal plant used extensively in Ayurvedic medicine as a natural rejuvenator and adaptogen. Its tubers are packed with a variety of bioactive compounds like flavonoids, alkaloids, and phenolic acids. Research has shown that these compounds contribute to their antioxidant, anti-inflammatory, liver-protecting, and anticancer properties (Madan & Karole, 2022) [21]. Similarly, *Jatropha gossypiifolia* L., locally called "Bi nidi zugu" in the Hausa tribe in Nigeria and a member of the *Euphorbiaceae* family, holds an important place in traditional African and South American healing practices. It has been traditionally used to treat infections, pain, inflammation, and tumors (Félix-Silva *et al*., 2014). The leaves of this plant are rich in compounds such as diterpenes, flavonoids, tannins, and saponins, many of which have demonstrated significant cytotoxic, anti-inflammatory, and antimicrobial effects.

While earlier studies have demonstrated the individual biological effects of *I. digitata* and *J. gossypiifolia*, there is still a lack of research looking into how these two plants might work together to provide enhanced anticancer and anti-inflammatory benefits particularly when delivered using advanced methods like nanocarriers to improve their effectiveness. Additionally, their potential to influence key cancer-related pathways such as NF-κB, Wnt/β-catenin, and MAPK signaling in colorectal cancer has yet to be thoroughly explored.

Building on this background, the study focused on encapsulating methanolic extracts of *I. digitata* tubers and *J. gossypiifolia* leaves within chitosan nanoparticles to explore their anticancer and anti-inflammatory effects against human colorectal cancer cell lines HCT116 and SW480. The objectives included: (i) characterizing the physicochemical properties of the extract-loaded chitosan nanoparticles; (ii) evaluating their cytotoxicity using MTT assays; (iii) assessing apoptosis induction through caspase-3 activity and Annexin V/PI staining; (iv) examining how these formulations influence NF-κB, Wnt/β-catenin, and MAPK signaling pathways via Western blotting and quantitative PCR; and (v) investigating their potential to reduce inflammation by measuring key pro-inflammatory cytokines.

This combined approach not only confirms the traditional medicinal value of *I. digitata* and *J. gossypiifolia* but also lays a solid scientific foundation for creating new plant-based nanomedicines to treat colorectal cancer. It highlights how addressing multiple cellular pathways at once can lead to better anticancer and anti-inflammatory effects, opening the door to more effective combination treatments down the line.

2. Materials and Methods
2.1 Materials
Low molecular weight chitosan (degree of deacetylation ~85%; Sigma-Aldrich, USA), sodium tripolyphosphate (TPP; Sigma-Aldrich, USA), methanol (HPLC grade; Merck, Germany), acetic acid (glacial, analytical grade; Merck, Germany), dimethyl sulfoxide (DMSO; Sigma-Aldrich, USA), Dulbecco's Modified Eagle's Medium (DMEM; Gibco, USA), fetal bovine serum (FBS; Gibco, USA), penicillin-streptomycin solution (100 U/mL and 100 µg/mL respectively; Gibco, USA), MTT reagent (3-(4,5-Dimethylthiazol-2-yl)-2,5-diphenyltetrazolium bromide; Sigma-Aldrich, USA), TRIzol reagent (Invitrogen, USA), cDNA synthesis kit (Thermo Fisher Scientific, USA), SYBR Green Master Mix (Applied Biosystems, USA), Annexin V-FITC/PI apoptosis detection kit (BD Biosciences, USA), caspase-3 colorimetric assay kit (Abcam, UK), primary antibodies against NF-κB p65, β-catenin, ERK1/2, p38 MAPK, COX-2, and GAPDH (Cell Signaling Technology, USA), HRP-conjugated secondary antibodies (Cell Signaling Technology, USA), ELISA kits for TNF-α and IL-6 (R&D Systems, USA), phosphate-buffered saline (PBS; pH 7.4; Gibco, USA), and Whatman No. 1 filter paper (GE Healthcare, UK).

All other chemicals and reagents used were of analytical grades purchased from trusted suppliers.

2.2 Methods
2.2.1 Collection of plant materials and extraction
Fresh tubers of *Ipomoea digitata* L. and leaves of *Jatropha gossypiifolia* L. were collected from the wild in Fori, Maiduguri in the evening hours in February 2025. They were authenticated by Dr. C.A. Ukwubile a taxonomist at the Department of Pharmacognosy, University of Maiduguri, Nigeria. The voucher specimen numbers (UMM/FPH/COV/004 and UMM/FPH/EUB/010) were deposited in the departmental herbarium. The plant

materials were washed, shade-dried for two weeks and pulverized into a fine powder using an electric grinder (M500, China). The powdered samples each weighing 800 g were cold macerated separately in 2.5 L of methanol in a separating funnel at room temperature for 72 h with intermittent shaking. The extracts were filtered through Whatman No. 1 filter paper, concentrated under reduced pressure using a rotary evaporator (Thermo Fisher Scientific, USA) at 40°C, and dried to obtain a semisolid extract. Their final weights were noted, and percentage yields were calculated concerning their initial weights (Lukiati *et al*., 2020) [20]. The extracts were then stored in a refrigerator at 4 °C until further when usage.

2.2.2 Phytochemical screening
A preliminary phytochemical screening was performed on the methanol extracts of the extracts to identify the presence of major groups of secondary metabolites. Standard qualitative tests were carried out to detect various compounds including alkaloids, flavonoids, tannins, saponins, phenolics, terpenoids, glycosides, and steroids (Al-Baaj & Abdul-Jalil, 2022) [1]. This approach helped provide an overview of the bioactive constituents present in the plant extracts.

2.2.2.1 Quantitative phytochemical analysis
Determination of total flavonoid content: To measure the total flavonoid content, we used the aluminium chloride colorimetric method. Briefly, 0.5 mL of the extract solution (at a concentration of 1 mg/mL) was combined with an equal volume (0.5 mL) of 2% aluminium chloride dissolved in methanol. This mixture was then left to react at room temperature for 30 minutes and kept in the dark to prevent any light interference. After incubation, the absorbance was read at 415 nm using a UV-visible spectrophotometer (Ezez *et al*., 2023) [6]. Quercetin served as the reference standard, and the flavonoid content was calculated and presented as milligrams of quercetin equivalent per gram of extract (mg QE/g extract).

Determination of total phenolic content: The total phenolic content was determined using the Folin–Ciocalteu reagent method. Specifically, 0.5 mL of extract (1 mg/mL) was combined with 2.5 mL of 10% Folin–Ciocalteu reagent. After a 5-minute waiting period, 2.0 mL of 7.5% sodium carbonate solution was added, and the mixture was incubated in the dark at room temperature for 30 minutes. Absorbance was then measured at 765 nm (Shah *et al*., 2022) [28]. Gallic acid was used as the standard, and results were expressed as milligrams of gallic acid equivalent per gram of extract (mg GAE/g extract).

Determination of total alkaloid content: The alkaloid content was measured using a modified Dragendorff's precipitation method. In this procedure, 1 g of the extract was dissolved in 20 mL of 10% acetic acid in ethanol and left to stand at room temperature for 4 hours. After filtration, concentrated ammonium hydroxide was added dropwise until complete precipitation took place. The resulting precipitate was then collected by filtration, washed with dilute ammonium hydroxide, dried, and weighed. Finally, the total alkaloid content was expressed as a percentage (w/w) of the extract (Alam *et al*., 2020) [3].

Determination of total tannin content: The total tannin content was measured using the Folin–Denis's method. To do this, 0.5 mL of the extract (at a concentration of 1 mg/mL) was mixed with 1.0 mL of Folin–Denis's reagent and 1.0 mL of saturated sodium carbonate solution. The

mixture was then diluted to 10 mL with distilled water and left to stand at room temperature for 30 minutes. After incubation, the absorbance was measured at 760 nm (Letaief *et al*., 2021) [16]. Tannic acid was used as the standard, and the tannin content was expressed as milligrams of tannic acid equivalent per gram of extract (mg TAE/g extract).

Determination of total saponin content: The total saponin content was measured using the vanillin–sulfuric acid colorimetric method. In this process, 0.5 mL of the extract (at a concentration of 1 mg/mL) was combined with 0.5 mL of 8% vanillin solution and 5.0 mL of 72% sulfuric acid. This mixture was then heated at 60°C for 10 minutes before being cooled down in an ice bath. The absorbance was recorded at 544 nm (El Sayed *et al*., 2020) [5]. Diosgenin was used as a reference standard, and the total saponin content was expressed as milligrams of diosgenin equivalent per gram of extract (mg DE/g extract).

2.2.3 Preparation of chitosan nanoparticles (CSNPs)
Chitosan nanoparticles encapsulating the plant extracts were prepared using ionic gelation. Briefly, a 1% (w/v) chitosan solution was made by dissolving 4 g of chitosan powder in 1% (v/v) acetic acid and then filtered. The plant extracts (1 g each) were first dissolved in 10 mL of ethanol, which was then added slowly into the chitosan solution while stirring continuously. Next, a 0.25% (w/v) tripolyphosphate (TPP) solution was added dropwise under constant stirring at 3000 rpm for 30 min using a 10 mL syringe, promoting nanoparticle formation through ionic crosslinking. The resulting nanoparticles were separated by centrifuging at 20,000 × g for 30 min and were washed twice with deionized water to remove any impurities (Javid *et al*., 2013; Maraicar & Narayanan, 2014; Raval *et al*., 2010; Younes & Rinaudo, 2015) [14, 23, 27, 36].

2.2.3.1 Characterization of CSNPs
Particle size, polydispersity index (PDI), and zeta potential of the CSNPs were measured by dynamic light scattering (DLS) using a Zetasizer Nano ZS (Malvern Instruments, UK), while morphological characteristics were examined through transmission electron microscopy (TEM). Encapsulation or drug entrapment efficiency (EE%) and loading capacity (LC%) of the prepared CSNPs were determined by quantifying the unencapsulated extract concentration using UV-visible spectroscopy at 230 nm. The *in vitro* release profile of the extracts from CSNPs was investigated using a dialysis tubing method, in which nanoparticles were suspended in phosphate-buffered saline (PBS, pH 7.4) and incubated at 37°C with constant agitation. At predetermined time intervals, aliquots were collected, centrifuged, and analyzed to determine the amount of released extract (Sultan *et al*., 2022) [29].

2.2.4 Cell culture
Human colorectal cancer cell lines HCT116 and SW480 were purchased from the American Type Culture Collection (ATCC, USA). The cells were grown in Dulbecco's Modified Eagle's Medium (DMEM) supplemented with 10% fetal bovine serum (FBS) and 1% penicillin-streptomycin. The cell cultures were maintained at 37°C in a humidified incubator with 5% CO_2.

2.2.5 Cytotoxicity evaluation by MTT assay
To assess the cytotoxic effects of the free extracts, blank chitosan nanoparticles (CSNPs), and extract-loaded CSNPs, we performed an MTT assay. Briefly, cells were seeded into 96-well plates at cell densities of 5,000 cells per well and allowed to grow overnight. The following day, the cells

were treated with different concentrations of the formulations, ranging from 5 to 100 µg/mL, for 24 hours. After treatment, 20 µL of MTT solution (5 mg/mL) was added to each well and incubated in a CO_2 incubator for an additional 4 hours to allow for formazan crystal formation. The crystals were then dissolved in DMSO. The absorbance was then measured at 570 nm using a microplate reader. From the resulting dose-response curves, the IC_{50} values were calculated (Madan & Karole, 2022) [21].

2.2.6 Apoptosis assay and caspase-3 activity

2.2.6.1 Apoptosis detection

Apoptosis detection was determined using an Annexin V-FITC/PI apoptosis detection kit, following the manufacturer's instructions (BD Biosciences, USA). Briefly, HCT116 and SW480 cells were plated in 6-well plates at a density of 2×10^5 cells per well and allowed to attach overnight. Thereafter, the cells were treated for 24 hours with either blank chitosan nanoparticles (CSNPs), free plant extracts as well as extract-loaded CSNPs, each at their respective IC_{50} concentrations. After treatment, both the floating and attached cells were collected, washed twice with cold phosphate-buffered saline (PBS, pH 7.4), and resuspended in 100 µL of 1× binding buffer. We then added 5 µL of Annexin V-FITC and 5 µL of propidium iodide (PI) to each sample, mixed them gently and incubated them for 15 minutes at room temperature in the dark. Following incubation, 400 µL of binding buffer was added, and the stained cells were immediately examined under a fluorescence microscope. Early apoptotic cells appeared green (Annexin V-positive/PI-negative), late apoptotic or necrotic cells showed both green and red fluorescence (Annexin V-positive/PI-positive), while live cells displayed no fluorescence (Annexin V-negative/PI-negative) (Alabsi et al., 2012) [2].

2.2.6.2 Caspase-3 activity

To further confirm that apoptosis was taking place, the activity of caspase-3, an enzyme that plays a key role in the process, was measured using a colorimetric assay kit (Abcam, UK). After treating the cells with test formulations for 24 h, we collected and washed them with PBS, then broke them open using the kit's lysis buffer to release their contents. The mixture was spun down at high speed (12,000 × g) for 10 min at 4 °C to separate the cell debris, and we collected the clear liquid on top for protein measurement using the Bradford assay. We then took equal amounts of protein (usually around 100 µg) and incubated it with a special substrate (DEVD-pNA) at 37°C for 1 to 2 h. When active caspase-3 was present, it cut this substrate, releasing a colored compound called p-nitroaniline (pNA) that can be quantified by measuring the absorbance at 405 nm with a microplate reader. By comparing these readings to untreated control cells, we were able to determine the level of caspase-3 activity. A higher absorbance indicates greater caspase-3 activation meaning the treatments were triggering apoptosis in the cancer cells (Ismail et al., 2025) [13].

2.2.7 Western blot analysis

Western blotting was carried out to evaluate the expression levels of key oncogenic and inflammatory signaling proteins such as NF-κB p65, β-catenin, ERK1/2, p38 MAPK, and COX-2. Briefly, HCT116 and SW480 cells were seeded in 6-well plates at a density of 3×10^5 cells/well and treated with extract-loaded CSNPs, free extracts, and blank CSNPs for 24 h at their respective IC_{50} concentrations. Thereafter, cells were washed twice with ice-cold PBS and lysed using

RIPA lysis buffer (containing protease and phosphatase inhibitors; Sigma-Aldrich, USA). The lysates were collected by centrifugation at 14,000 rpm for 10 min at 4°C. Protein concentration was then evaluated using the Bradford assay (Bio-Rad, USA). Equal amounts of protein (30-50 µg) were separated on 10-12% SDS-PAGE gels and subsequently transferred onto polyvinylidene difluoride (PVDF) membranes (Millipore, USA) using a semi-dry transfer system (Bio-Rad, USA). Membranes were blocked with 5% non-fat dry milk in Tris-buffered saline containing 0.1% Tween-20 (TBS-T) for 1 h at room temperature to prevent non-specific binding. Blocked membranes were then incubated overnight at 4°C with primary antibodies specific for NF-κB p65, β-catenin, ERK1/2, p38 MAPK, COX-2, and GAPDH (which served as internal loading control) at dilutions of 1:1000. After washing three times with TBS-T, membranes were incubated with HRP-conjugated secondary antibodies (1:5000 dilution) for 1 h at room temperature. Protein bands were visualized using an enhanced chemiluminescence (ECL) detection kit (Thermo Fisher Scientific, USA) and captured with a ChemiDoc imaging system (Bio-Rad, USA). Densitometric analysis of protein bands was performed using ImageJ software (NIH, USA), and results were normalized against GAPDH expression. The relative fold change in expression compared to untreated control cells was calculated (Guo & Liu, 2021) [11].

2.2.8 Quantitative real-time PCR (qRT-PCR)

Quantitative real-time PCR (qPCR) was used to measure the mRNA levels of several key genes involved in cancer progression and inflammation, such as NF-κB p65, β-catenin, ERK1/2, p38 MAPK, and COX-2. Briefly, HCT116 and SW480 cells were treated for 24 hours with either blank chitosan nanoparticles (CSNPs), free extracts, and extracts loaded into CSNPs each at their respective IC_{50} concentrations. After treatment, we isolated the total RNA from the cells using a TRIzol reagent, following the manufacturer's guidelines. We then assessed the purity and concentration of the RNA samples using a NanoDrop spectrophotometer, only moving forward with samples that had an A260/A280 ratio between 1.8 and 2.0 to ensure quality. Next, we converted 1 microgram of this RNA into complementary DNA (cDNA) using a commercial cDNA synthesis kit. The cDNA served as the template for our qPCR reactions, which were performed using SYBR Green Master Mix on a real-time PCR system. Each qPCR reaction had a total volume of 20 µL, containing the master mix, gene-specific forward and reverse primers, cDNA template, and nuclease-free water. The primers were carefully designed for each target gene and synthesized commercially. To make sure we had a reliable comparison, the housekeeping gene GAPDH was used as an internal control to normalize the expression data (Guo & Liu, 2021) [11].

2.2.9 Inflammatory cytokines using ELISA (anti-inflammatory evaluation)

To evaluate the anti-inflammatory effects of the formulations, we measured the levels of key inflammatory molecules tumor necrosis factor-alpha (TNF-α), interleukin-6 (IL-6), and cyclooxygenase-2 (COX-2) in the culture media of treated HCT116 and SW480 cells using commercial ELISA kits. Briefly, cells were seeded in 6-well plates at a density of 300,000 cells per well. The cells were then treated for 24 h with either blank CSNPs, free plant extracts, or plant extracts loaded into CSNPs, each at their

respective IC_{50} doses. After treatment, we collected the culture supernatants and spun them down at $3,000 \times g$ for 10 min to clear out any leftover cell debris. These clean samples were then frozen at –80°C until we were ready for analysis. For the ELISA tests, we followed the manufacturer's instructions closely. That is, 100 µL of each sample or standard solution was added to 96-well plates that were already coated to capture the specific cytokines. The plates were incubated at room temperature for 2 hours to allow the targets to bind. After washing away unbound substances, we added biotin-linked detection antibodies and incubated them for another 1 h. Following a second wash, we introduced HRP-conjugated streptavidin and let it incubate for 45 minutes. Next, we added a TMB substrate solution to each well and let the color develop in the dark for 20 minutes. To stop the reaction, 50 µL of a stop solution (2N H_2SO_4) was added, turning yellow. The absorbance was then measured at 450 nm with a microplate reader, which allowed us to determine the concentrations of TNF-α, IL-6, and COX-2 by comparing the readings against standard curves prepared for each cytokine. All measurements were done in triplicate to ensure accuracy, and the results were reported as picograms per millilitre (pg/mL) (Kandilarov et al., 2023) [15].

2.2.10 Experimental animals for in vivo anti-inflammatory evaluation

Wistar rats weighing 150-200 g were sourced from the Department of Human Physiology at Ahmadu Bello University, Zaria, Nigeria. Male Swiss albino mice, weighing between 50-80 g, were also obtained from the same department. The animals were housed in a room with controlled temperature and humidity (24 °C and 65% air humidity). They were given unlimited access to a standard diet and water. Before the experiment, the animals were placed individually in metabolic cages without food but with free access to water for 12 hours. All experimental protocols complied with the National Institutes of Health Guidelines for the Care and Use of Laboratory Animals.

2.2.10.1 Carrageenan-induced rats' paw edema

The anti-inflammatory activity of extracts was evaluated using the carrageenan-induced paw edema model in rats following the method described by Ukwubile (2024) [31]. In all groups, inflammation and swelling were induced by injecting 0.1 mL of a freshly prepared 1% carrageenan suspension into the right hind paw's footpad. The left hind paw was left untreated to serve as a control for measuring changes in paw thickness. Carrageenan injection led to visible redness and significant swelling, becoming prominent after 3 hours and lasting throughout the experiment. Paw edema was measured at 0, 1, 2, 3, 4, and 5-hour intervals using a Vernier digital caliper. Rats were divided into five groups of six animals each. One hour before carrageenan injection, three groups were pretreated with the extracts at doses of 100, 200, and 400 mg/kg respectively. The remaining two groups received either distilled water (vehicle control, 10 mL/kg) or diclofenac (10 mg/kg) as a reference drug. The percentage inhibition of edema was calculated by comparing paw thickness changes (difference between the untreated left paw and treated right paw) in the treated groups relative to the vehicle control (Ukwubile, 2024) [31].

$$Inhibition\ (\%) = \frac{Paw\ volume\ in\ control - paw\ volume\ in\ treatment}{Paw\ volume\ in\ control} \times 100 \quad (1)$$

2.2.10.2 Xylene–induced mice ear edema

A total of 35 male Swiss albino mice, each weighing between 50 and 80 g, were randomly divided into five groups: a model group serving as the negative control, a dexamethasone-treated group as the positive control, and three groups receiving low, medium, and high doses of the extracts (including both free plant extracts and chitosan nanoparticle-loaded extracts). For the methanol extract, the low, medium, and high dose groups were administered 200, 400, and 800 mg/kg/day (body weight), respectively. Similarly, another set of methanol extract doses were 20, 40, and 80 mg/kg/day. Dexamethasone was given at 6 mg/kg/day to both extract groups as a positive control. All test substances, including extracts and dexamethasone, were delivered orally via gavage at a dosage volume of 0.2 mL per 10 g of body weight, using normal saline as the vehicle. The negative control group received 2 mL of normal saline once daily. After five days of treatment, 0.1 mL of xylene was applied evenly on both the inner and outer surfaces of the right ear of each mouse to induce edema, while the left ear remained untreated as a control. Four hours later, the animals were euthanized, and their ears were excised along the margin. Using a 6 mm stainless steel punch, ear tissue samples were taken from the corresponding regions of both ears of each mouse. These ear discs were then weighed using an analytical balance. The level of edema was determined by calculating the weight difference between the treated right ear and the untreated left ear within the same animal. The percentage of edema inhibition was used as a measure of the anti-inflammatory effects of the extracts. Finally, the ear tissues were stored at -60°C for further analysis (Oppong et al., 2024) [25].

2.2.10.3 Evaluation of inflammatory markers level in the rats' paw

The levels of TNF-α, IL-1β, NO, and COX-2 in paw tissues were measured using the ELISA method, following the method previously described by Van Der Willik et al. (2018) [33] with modifications. Five hours after inflammation was induced, the paw tissue samples were collected, weighed, and stored at −15 °C until analysis. The subcutaneous tissue from the right hind paw and the area around the torso-tibial joints were homogenized in phosphate-buffered saline (PBS) at pH 7.4. The homogenates were then centrifuged at 10,000 rpm for 10 minutes at 4°C. The resulting supernatants were analyzed by ELISA according to the manufacturer's guidelines to determine the levels of TNF-α, IL-1β, NO, and COX-2. In brief, ELISA microtiter plates pre-coated with monoclonal antibodies specific to each cytokine were used. The homogenate samples were added to the wells, and after washing away unbound substances, a secondary biotinylated polyclonal antibody was applied. This antibody was detected by a streptavidin-peroxidase conjugate, leading to a color change upon the addition of the substrate. After stopping the color development, absorbance was measured at 490 nm using an ELISA reader. Concentrations of each parameter were then determined by comparison with standard curves (Van Der Willik et al., 2018) [33].

2.2.11 Statistical analysis

Data obtained were expressed as mean ± SD (n = 3). Statistical significance was assessed using one-way ANOVA followed by Tukey's post hoc test. A p-value < 0.05 or 0.001 was considered statistically significant. All

experiments were performed in triplicate. Analysis was done using GraphPad Prism version 9.0 statistical software.

3. Results

3.1 Phytochemical content
A phytochemical analysis of the methanol extracts showed that both *I. digitata* tubers and *J. gossypiifolia* leaves contain a variety of compounds, including alkaloids, flavonoids, phenolics, saponins, tannins, glycosides, terpenoids, and steroids. Interestingly, anthraquinones were found only in *J. gossypiifolia* and were absent in *I. digitata*. This difference in their chemical makeup hints at unique properties that might explain the different biological effects they exhibit (Table 1). Similarly, the results also indicate that their total phenolic and flavonoid contents were greater than those of alkaloids, saponins, and tannin contents (Table 2).

Table 1: Phytochemical content of methanol extracts of *I. digitata* tubers and *J. gossypiifolia* leaves

Phytochemical	Test	*I. digitata* tubers	*J. gossypiifolia* leaves
Alkaloids	Dragendorff's	+	+
Flavonoids	Shinoda	+	+
Phenolics	Ferric chloride	+	+
Saponins	Froth formation	+	+
Tannins	Ferric chloride	+	+
Glycosides	Keller-Kiliani	+	+
Terpenoids	Salkowski	+	+
Steroids	Liebermann-Burchard	+	+
Anthraquinones	Borntrager's	-	+

Note: + denotes detected or present, and – denotes not detected or absent

Table 2: Quantitative phytochemicals of methanol extracts of *I. digitata* tubers and *J. gossypiifolia* leaves

Phytochemical	Test	*I. digitata* (mg/g)	*J. gossypiifolia* (mg/g)
Phenolics	Folin–Ciocalteu	52.6 ± 1.8	48.3 ± 2.1
Flavonoids	Aluminum chloride colorimetric	38.4 ± 1.2	41.7 ± 1.5
Saponins	Vanillin–sulfuric acid	24.2 ± 0.9	26.5 ± 1.0
Alkaloids	Dragendorff's	17.3 ± 0.7	19.8 ± 0.6
Tannins	Folin–Denis	31.5 ± 1.4	29.2 ± 1.3

Note: total phenolic and flavonoid contents are expressed in mg GAE/g and mg QE/g respectively

3.2 Characterization of extract-loaded chitosan nanoparticles
The methanol extracts from the tubers of *I. digitata* and the leaves of *J. gossypiifolia* were successfully loaded into chitosan nanoparticles using the ionic gelation method. When we measured the particle sizes using dynamic light scattering (DLS), the plain chitosan nanoparticles without any extract had an average size of about 160 ± 5.0 nm. After adding the extracts, the particles grew slightly larger, averaging around 180 ± 7.0 nm, which confirms that the extracts were effectively encapsulated. Additionally, the polydispersity index (PDI) stayed below 0.3, indicating that the nanoparticles were uniform in size and well-distributed (Fig 1a). Similarly, transmission electron microscopy (TEM) images (Fig 1b), showed that the nanoparticles were

nicely round with smooth surfaces, and their sizes matched well with the results from dynamic light scattering (DLS) measurements. Additionally, the extract-loaded chitosan nanoparticles demonstrated high encapsulation efficiency, capturing over 85% of the extract, while the amount of extract loaded made up about 10% of the nanoparticle's total weight.
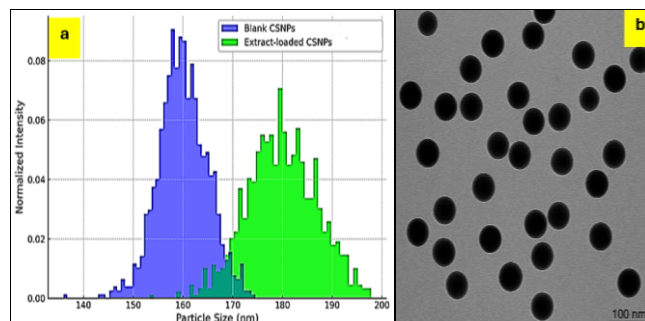

Fig 1: Particle size (chitosan and extract-loaded CSNPs) and morphology of extract-loaded CSNPs

3.3 Physicochemical properties of formulated CSNPs
We successfully encapsulated methanol extracts from *I. digitata* tubers and *J. gossypiifolia* leaves into chitosan nanoparticles using the ionic gelation method. The process was quite efficient, with over 85% of the bioactive compounds being well entrapped within the nanoparticles. The loading capacity was around 10%, indicating a good balance between the extract and the chitosan polymer. We achieved a production yield of 78%, which shows that the method is reliable and can be scaled up if needed. When tested in the lab, the nanoparticles released about 65% of the extracts gradually over 24 hours, highlighting their ability for controlled, sustained release. Additionally, the nanoparticles had a swelling index of 120%, meaning they could absorb water well which is beneficial for maintaining a steady release of the physiological pH (Table 3).

Table 3: Physicochemical properties of *I. digitata* and *J. gossypiifolia* extract-loaded CSNPs

Parameter	Result (mean $\pm$ SD)
Encapsulation efficiency (EE)	86.4 ± 2.3 %
Loading capacity (LC)	10.2 ± 0.8 %
Production yield	78.5 ± 1.9 %
In vitro release (24 hours)	65.3 ± 3.1 %
Swelling index	120.7 ± 4.2 %

Results are mean $\pm$ SD (n = 3)

3.4 In vitro release profile of extract-loaded CSNPs
The *in vitro* release study showed that the extract-loaded chitosan nanoparticles (IDJG1-IDJG4), steadily released the extract over 24 hours. About 15% of the extract was released quickly within the first 2 hours, with an initial burst followed by a slow and controlled release that reached roughly 65% after 24 hours for formulation IDJG1 (Fig 2). This gradual release pattern suggests that the CSNPs can maintain effective levels of extract in the body for a longer time, making them promising candidates for use in colorectal cancer treatment.
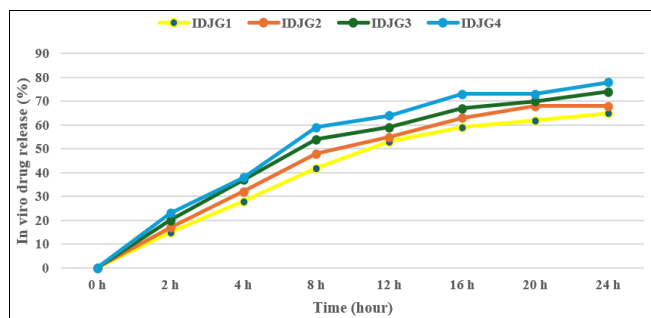
Fig 3: *In vitro release* profiles of formulations IDJG1-IDJG4 in 24 hours. Note: IDJG1 was used for targeted delivery in this study

3.5 Cytotoxic effects of extract-loaded CSNPs on HCT116 and SW480 cells

We tested how well blank chitosan nanoparticles (CSNPs), free plant extracts, and extract-loaded CSNPs could kill two types of colorectal cancer cells (HCT116 and SW480) using the MTT assay after 24 hours. The blank CSNPs were very gentle on the cells, keeping more than 90% of them alive, which confirms that these nanoparticles are biocompatible and not harmful on their own. The free extracts from the plants *I. digitata* and *J. gossypiifolia* showed moderate ability to kill cancer cells, with IC_{50} values (the concentration needed to kill half the cells) between 45 and 58 µg/mL. However, when these extracts were loaded onto the CSNPs, their cancer-killing power improved significantly, with IC_{50} values dropping to between 22 and 35 µg/mL, depending on the cell type and which plant extract was used. For instance, the *I. digitata*-loaded CSNPs had IC_{50} values of about 24.6 µg/mL for HCT116 cells and 28.3 µg/mL for SW480 cells. Similarly, *J. gossypiifolia*-loaded CSNPs had values of 22.5 µg/mL for HCT116 and 26.7 µg/mL for SW480. This clearly shows that loading the extracts onto CSNPs enhances their ability to kill colorectal cancer cells (Table 4). Similarly, when viewed under an inverted microscope, the treated cells showed clear signs of apoptosis, specifically in HCT116 cells. These included noticeable cell shrinkage, membrane blebbing, and chromatin condensation, with these features being especially prominent in the groups treated with extract-loaded CSNPs (Fig 4).

Table 4: Cytotoxic effects of CSNPs-loaded with extracts of *I. digitata* and *J. gossypiifolia* against HCT116 and SW480 cells

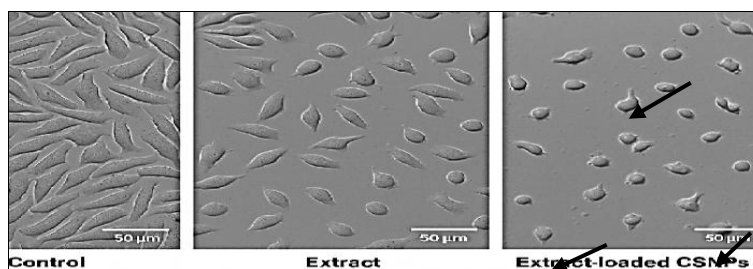| Sample	Cell type	IC$_{50}$ (µg/mL)	Cell morphology
Blank CSNPs	HCT116	>100 (Viability >90%)	Normal morphology
Blank CSNPs	SW480	>100 (Viability >90%)	Normal morphology
Free *I. digitata* extract	HCT116	48.7 ± 2.5	Mild apoptosis
Free *I. digitata* extract	SW480	53.2 ± 2.9	Mild apoptosis
Free *J. gossypiifolia* extract	HCT116	45.3 ± 2.1	Mild apoptosis
Free *J. gossypiifolia* extract	SW480	50.8 ± 2.6	Mild apoptosis
I. digitata-loaded CSNPs	HCT116	24.6 ± 2.1	Strong apoptosis
I. digitata-loaded CSNPs	SW480	28.3 ± 1.7	Strong apoptosis
J. gossypiifolia-loaded CSNPs	HCT116	22.5 ± 1.9	Strong apoptosis
J. gossypiifolia-loaded CSNPs	SW480	26.7 ± 2.2	Strong apoptosis

Fig 4: Photomicrographs of colorectal cancer cells HCT116 cells treated with extract-loaded CSNPs showing chromatin condensation (arrows)

3.6 Induction of apoptosis and caspase-3 activation

After evaluating apoptosis induction by treating the cells with extract-loaded CSNPs using Annexin V-FITC/PI dual staining combined with fluorescence microscopy, the results showed that in both HCT116 and SW480 cell lines, treatment with the extract-loaded CSNPs led to a significant ($p < 0.05$), increase in the number of cells undergoing early and late apoptosis, compared to those treated with free extracts or blank CSNPs (Fig 5). Quantitative analysis showed a remarkable increase in the percentage of apoptotic cells after treatment with the extract-loaded CSNPs. In HCT116 cells, apoptosis rose from just 8.2% in the untreated control group to 46.5% with *I. digitata*-loaded CSNPs and 49.1% with *J. gossypiifolia*-loaded CSNPs ($p < 0.001$) (Fig 5a). A similar pattern was seen in SW480 cells, where apoptosis rates reached 44.8% and 47.6% for the two respective treatments. In contrast, cells treated with the free extracts experienced much lower apoptosis levels, around 28–30% (Fig 5b).

Similarly, fluorescence microscopy images revealed bright green (Annexin V) and red (PI) signals in the treated groups, highlighting the exposure of phosphatidylserine on the cell surface and changes in membrane permeability that are characteristic of apoptosis (Fig 6). Additionally, the activity of caspase-3, an essential enzyme involved in carrying out apoptosis, was significantly higher in cells treated with extract-loaded CSNPs. Compared to untreated cells (control), caspase-3 activity increased by about 3.5 times in cells treated with *I. digitata*-loaded CSNPs and by 4 times in those treated with *J. gossypiifolia*-loaded CSNPs ($p < 0.001$). Similar results were observed in SW480 cells, supporting the idea that the extracts loaded into CSNPs trigger apoptosis through the activation of caspase-3 (Fig 7).
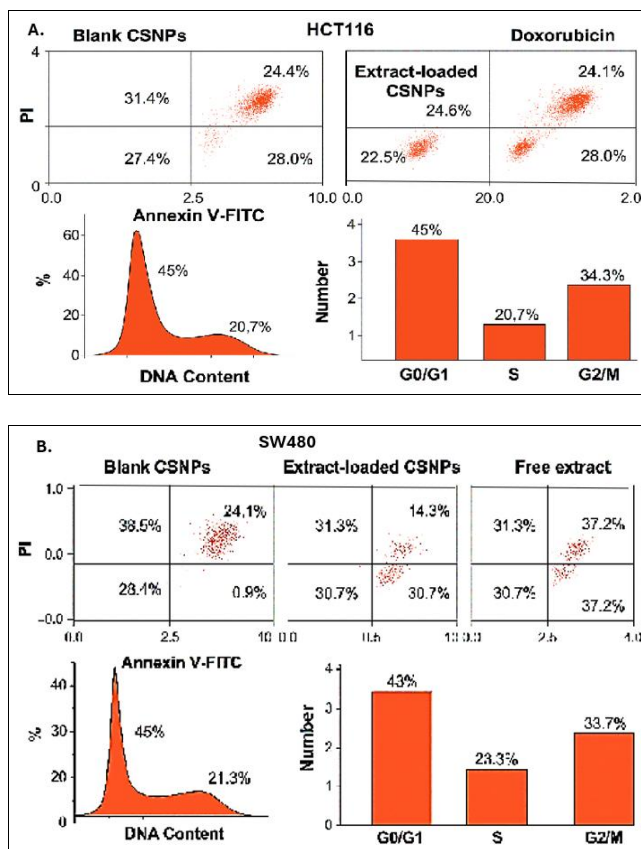
Fig 5: Induction of apoptosis and cell cycle arrest in HCT116 (A) and SW480 (B) colorectal cancer cells following treatment with extract-loaded CSNPs and doxorubicin as measured by Annexin V-FITC/PI dual staining. Note: The upper panels display Annexin V-FITC/PI staining, revealing increased apoptosis in treated cells vs controls. The bottom left panel shows DNA content histograms with a notable rise in Sub-G1 phase cells, indicating apoptosis. The bottom right panel summarizes cell cycle distribution across G0/G1, S, and G2/M phases
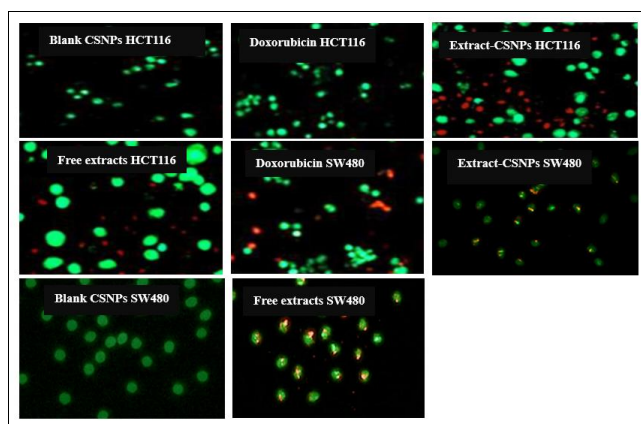

Fig 6: Fluorescence microscopy analysis of apoptosis in HCT116 and SW480 colorectal cancer Cells treated with various treatments
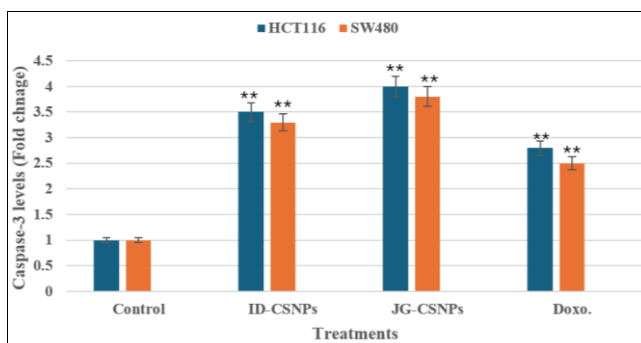

Fig 7: Effects on caspase-3 activity by various treatments on HCT116 and SW480 colorectal cancer cells. Values are expressed as mean ± SD (n = 3). ** Statistically significant at $p < 0.001$ vs. control (one-way ANOVA followed by Turkey's post hoc test). Caspase-3 activity was measured using a fluorometric assay and expressed as fold change relative to untreated control. ID-CSNPs: *I. digitata*-loaded CSNPs, JG-CSNPs: *J. gossypiifolia*-loaded CSNPs and Doxo.: doxorubicin

3.7 Inhibition of oncogenic signaling pathways

To better understand how the extract-loaded CSNPs fight cancer, we looked at the levels of important proteins that drive colorectal cancer growth, specifically NF-κB p65, β-catenin, ERK1/2, and p38 MAPK. We measured these proteins using Western blotting and quantitative PCR techniques. The results showed that treating the cancer cells with CSNPs loaded with *I. digitata* and *J. gossypiifolia* extracts led to a significant decrease in the levels of NF-κB p65 and β-catenin proteins in both HCT116 and SW480 cell lines (Fig 8 A). This reduction was much greater compared to cells that were untreated or treated with the free extracts alone. Detailed analysis revealed that NF-κB p65 levels dropped by about 65%, while β-catenin levels decreased by around 60% after treatment with the CSNPs (p < 0.001).

Likewise, the activated forms of ERK1/2 and p38 MAPK proteins that play important roles in helping tumor cells survive and grow were noticeably reduced. In fact, the levels of these phosphorylated proteins dropped by about 55% and 50%, respectively, after treatment with the extract-loaded CSNPs compared to untreated cells. Matching the results obtained from the Western blot, the qPCR tests also showed a clear drop in the mRNA levels of NF-κB, CTNNB1 (β-catenin), ERK1/2, and p38 MAPK genes (Fig 8 B). This confirms that the treatments were effectively blocking these targets not just at the protein level but also by reducing their gene expression.
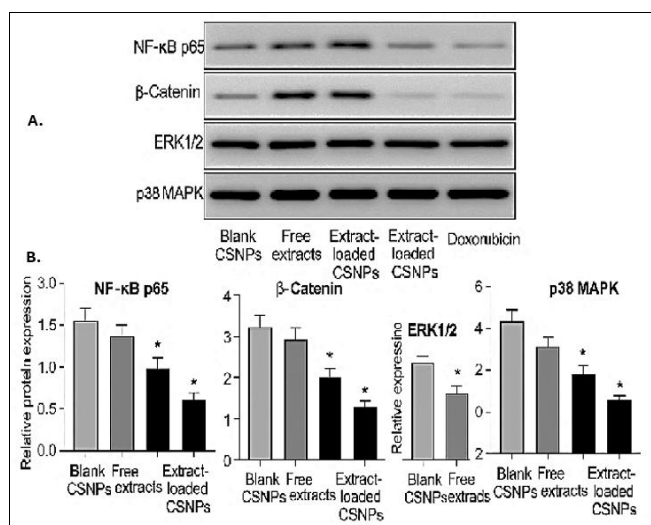

Fig 8: Molecular analysis of oncogenic signaling pathways following treatment with extract-loaded CSNPs in HCT116 and SW480 cells. (A) Western blot analysis confirming the corresponding reduction in protein expression of NF-κB p65, β-catenin, ERK1/2, and p38 MAPK following treatment, and (B) Quantitative PCR (qPCR) analysis showing relative mRNA expression levels of NF-κB p65, β-catenin, ERK1/2, and p38 MAPK. Gene expression levels were normalized using GAPDH as an internal control and are presented as fold changes relative to the control group. The data are shown as the mean ± SD (n = 3). * Statistically significant at p < 0.001 (one-way ANOVA)

3.8 Anti-inflammatory effects via suppression of TNF-α, IL-6, and COX-2

We evaluated the anti-inflammatory effects of extract-loaded CSNPs by measuring key pro-inflammatory molecules tumor necrosis factor-alpha (TNF-α), interleukin-6 (IL-6), and cyclooxygenase-2 (COX-2) in treated HCT116 and SW480 cells using ELISA. Treatment with CSNPs loaded with *I. digitata* and *J. gossypiifolia* extracts led to a significant decrease in TNF-α and IL-6 levels compared to both untreated cells and those treated with free extracts (p < 0.001). Specifically, in HCT116 cells, TNF-α levels dropped by about 58%, while IL-6 decreased by around 54% after CSNP treatment. Similar reductions were seen in SW480 cells, with TNF-α and IL-6 levels falling by approximately 55% and 52%, respectively (Table 5). Additionally, treatment with the extract-loaded CSNPs significantly lowered COX-2 levels in the cells, both in terms of the protein and the gene's activity. Western blot results showed that COX-2 protein expression dropped by about 60%, and qPCR confirmed a similar decrease in COX-2 mRNA levels (Table 6).

Table 5: Effect of extract-loaded CSNPs on pro-inflammatory cytokines production

Treatment	TNF-α reduction (%)	IL-6 reduction (%)
HCT116 control (untreated)	0	0
HCT116 free extract	32	30
HCT116 extract-loaded CSNPs	58	54
SW480 control (untreated)	0	0
SW480 free extract	29	28
SW480 extract-loaded CSNPs	55	52

Table 6: COX-2 expression after treatments

Treatment	%COX-2 protein reduction	%COX-2 mRNA reduction
HCT116 control (untreated)	0	0
HCT116 free extract	33	31
HCT116 extract-loaded CSNPs	60	59
SW480 control (untreated)	0	0
SW480 free extract	30	28

3.9 In vivo anti-inflammatory studies

3.9.1 Effects on carrageenan-induced paw edema

Using the carrageenan-induced paw edema model, we found that both *I. digitata* and *J. gossypiifolia* extracts, when delivered through chitosan nanoparticles (ID-CSNPs and JG-CSNPs), significantly reduced inflammation in rat paws, with stronger effects seen at higher doses. At 3 and 5 hours after inducing inflammation, the ID-CSNPs at 400 mg/kg showed the most pronounced anti-inflammatory effect, reducing swelling by 47.42% and 53.57%, respectively. Similarly, the JG-CSNPs at the same dose reduced edema by 43.21% and 49.12% at those time points. These results were comparable to those seen with diclofenac (p < 0.01), a standard anti-inflammatory drug, which achieved 50.23% and 56.89% inhibition. While the free plant extracts and blank nanoparticles also helped reduce swelling, their effects were noticeably smaller, highlighting how formulating the extracts into nanoparticles improved their anti-inflammatory performance (Table 7).

Table 7: Effect of extracts and CSNPs on carrageenan-induced paw edema in rats

Treatment group	Paw thickness (3h) (mm)	Inhibition (%)	Paw thickness (5h) (mm)	Inhibition (%)
Normal Control	4.21 ± 0.12	–	4.45 ± 0.13	–
Free CSNPs	3.69 ± 0.15	12.34 ± 0.67	3.82 ± 0.14	14.25 ± 0.71
IDE (100 mg/kg)	3.18 ± 0.11*	24.56 ± 1.25*	3.17 ± 0.13*	28.78 ± 1.30*
IDE (200 mg/kg)	2.70 ± 0.10*	35.87 ± 1.13*	2.65 ± 0.12*	40.54 ± 1.21*
ID-CSNPs (400 mg/kg)	2.21 ± 0.09**	47.42 ± 1.05**	2.06 ± 0.08**	53.57 ± 1.02**
JGE (100 mg/kg)	3.31 ± 0.13*	21.45 ± 1.22*	3.32 ± 0.14*	25.67 ± 1.24*
JGE (200 mg/kg)	2.91 ± 0.12*	30.76 ± 1.19*	2.81 ± 0.11*	36.78 ± 1.15*
JG-CSNPs (400 mg/kg)	2.40 ± 0.10**	43.21 ± 1.08**	2.27 ± 0.09**	49.12 ± 1.07**
Diclofenac (10 mg/kg)	2.09 ± 0.09**	50.23 ± 0.98**	1.92 ± 0.08**	56.89 ± 0.95**

* $p < 0.05$, ** $p < 0.01$ vs. normal control group using one-way ANOVA followed by Turkey's post hoc test. ID-CSNPs: *I. digitata* extract loaded CSNPs, IDE: Free extract, JG-CSNPs: *J. gossypiifolia* extract loaded CSNPs, and JGE: Free extract

Table 8: Effect of extract-loaded CSNPs and controls on xylene-induced ear edema in mice

Treatment group	Ear edema (mg)	Inhibition (%)
Normal control	10.25 ± 0.62	0.00
Free CSNPs	9.84 ± 0.51	3.99
IDE (800 mg/kg)	7.92 ± 0.48*	22.68*
ID-CSNPs (800 mg/kg)	6.15 ± 0.42**	40.00**
JGE (800 mg/kg)	8.03 ± 0.46*	21.66*
JG-CSNPs (800 mg/kg)	6.42 ± 0.39**	37.37**
Dexamethasone (6 mg/kg)	5.87 ± 0.33**	42.73**

* $p < 0.05$, ** $p < 0.001$ compared to normal control (one-way ANOVA). ID-CSNPs: *I. digitata* extract loaded CSNPs, IDE: Free extract, JG-CSNPs: *J. gossypiifolia* extract loaded CSNPs, and JGE: Free extract. Results are shown as the mean ± SD (n = 3)

3.9.2 Effects on xylene–induced mice ear edema

When given to mice, the extract-loaded chitosan nanoparticles (ID-CSNPs and JG-CSNPs) significantly eased ear swelling caused by xylene, performing better than both the free extracts and untreated controls. At a dose of 800 mg/kg, ID-CSNPs and JG-CSNPs showed strong anti-inflammatory effects, reducing swelling by 40.00% and 37.37%, respectively, results that were very close to those of dexamethasone, a common anti-inflammatory medication, which achieved 42.73% swelling reduction (Table 8). On the other hand, the free extracts (IDE and JGE) only moderately lowered inflammation, with inhibition rates around 22%, while the nanoparticles without any extract had little impact. Overall, these findings suggest that packaging the extracts into chitosan nanoparticles significantly boosts their ability to fight acute inflammation.

3.9.3 Effects on inflammatory markers level in the rats' paw

Giving rats the extract-loaded chitosan nanoparticles (ID-CSNPs and JG-CSNPs) led to a significant drop in key inflammation markers like TNF-α, IL-1β, nitric oxide (NO), and COX-2 in their paw tissues. These nanoparticles outperformed both the free extracts and the nanoparticles without extracts. In particular, at a dose of 400 mg/kg, ID-CSNPs and JG-CSNPs brought these inflammatory markers down close to the levels seen in healthy rats, highlighting a strong anti-inflammatory effect (Table 9). This suggests that the nanoparticles help reduce inflammation by lowering the activity of molecules that promote it.

Table 9: Effects of extracts and extract-loaded CSNPs on inflammatory markers in rat paw tissue

Treatment group	TNF-α (pg/mg protein)	IL-1β (pg/mg protein)	NO (μM)	COX-2 (pg/mg protein)
Normal control	22.10 ± 1.25	15.85 ± 0.98	30.10 ± 2.10	18.70 ± 1.12
Free CSNPs	28.45 ± 1.78	21.40 ± 1.22	42.30 ± 2.55	27.60 ± 1.45
IDE (400 mg/kg)	24.80 ± 1.32*	17.90 ± 1.00*	35.20 ± 1.90*	21.90 ± 1.25*
ID-CSNPs (400 mg/kg)	18.45 ± 1.14**	13.20 ± 0.87**	25.50 ± 1.60**	16.10 ± 0.95**
JGE (400 mg/kg)	25.60 ± 1.45*	18.45 ± 0.95*	36.10 ± 1.85*	22.30 ± 1.20*
JG-CSNPs (400 mg/kg)	19.30 ± 1.20**	13.80 ± 0.90**	26.30 ± 1.75**	16.75 ± 0.98**

* $p < 0.05$, ** $p < 0.001$ vs. free CSNPs group (one-way ANOVA). ID-CSNPs: *I. digitata* extract loaded CSNPs, IDE: Free extract, JG-CSNPs: *J. gossypiifolia* extract loaded CSNPs, and JGE: Free extract. Results are shown as the mean ± SD (n = 3)

4. Discussion

The present study explored the therapeutic potential of chitosan nanoparticles (CSNPs) encapsulating *Ipomoea digitata* (ID) tuber and *Jatropha gossypiifolia* (JG) leaf methanol extracts in colorectal cancer (CRC) models, focusing on the HCT116 and SW480 cell lines. The plant-based nano formulations were found to significantly inhibit cell proliferation, induce apoptosis, modulate key pro-inflammatory and oncogenic signaling pathways, and reduce inflammatory responses. These findings highlight the multifaceted anticancer and anti-inflammatory properties of the formulations. Furthermore, the results align with and extend existing ethnopharmacological evidence supporting the traditional use of these plants in managing inflammation and cancer-related conditions (Madan & Karole, 2022) [21].

Encapsulating the plant extracts in chitosan nanoparticles (CSNPs) significantly boosted their effectiveness, especially by improving how well the cells took them up and how steadily the extracts were released over time. This was clearly shown through detailed imaging studies. The nanoparticles containing *I. digitata* and *J. gossypiifolia* extracts were much better at slowing the growth of colorectal cancer cells (HCT116 and SW480) than the extracts on their own. When we looked at cell death using flow cytometry, nearly 45% of SW480 cells treated with the nanoparticle-encapsulated extracts underwent apoptosis, compared to only about 28–30% with the free extracts. A similar trend was observed in HCT116 cells. These results

suggest that packaging the extracts into nanoparticles greatly enhances their potency, likely by making them more stable, easier to dissolve, and more efficiently delivered inside the cells, consistent with what other studies on chitosan nanoparticle-based plant therapies have found (Wei *et al*., 2021) [34].

Through its analysis, this study demonstrates strong proof that intrinsic apoptotic pathway activation causes the antiproliferative effects observed. Analysis shows that Caspase-3 activity increased significantly to 3.5 times in ID-CSNP-treated HCT116 cells and 4.0 times in JG-CSNP-treated cells compared to untreated controls which suggests mitochondrial-dependent cell death as the likely mechanism. The findings match previous research showing plant extract-loaded nanoparticles induce caspase activation during cancer treatment (Herdiana *et al*., 2022) [12]. Our study investigated the impact of nano formulations on the molecular mechanisms that drive colorectal cancer development. The expression of NF-κB, Wnt/β-catenin, and MAPK signaling pathways decreased significantly after treatment with extract-loaded CSNPs according to Western blot and immunofluorescence analysis. The NF-κB, Wnt/β-catenin, and MAPK signaling pathways demonstrate overactive behavior in colorectal cancer (CRC) while advancing cellular proliferation and inflammation and enabling angiogenesis and apoptotic resistance (Grivennikov *et al*., 2010; Madan & Karole, 2022; Oppong *et al*., 2024; Paramee *et al*., 2018; Ukwubile *et al*., 2025) [10, 21, 25, 26, 32]. The nano formulations' anticancer effects work by disrupting essential signal transduction cascades for tumor cell survival as shown by the suppressed phosphorylation of ERK, JNK, and p38 MAPK proteins.

Beyond the *in vitro* setting, the anti-inflammatory potential of ID-CSNPs and JG-CSNPs was validated in two well-established animal models: carrageenan-induced paw edema and xylene-induced ear edema. The nano formulations demonstrated significant edema reduction which matched the efficacy of diclofenac and dexamethasone in both test models. The ID-CSNPs and JG-CSNPs at 400 mg/kg dosage resulted in more than 60% edema inhibition at 5 hours in the carrageenan model which outperformed free extracts and vehicle controls. The anticancer effect appears to be influenced by inflammation suppression which is relevant because chronic inflammation has a well-established connection to colorectal cancer development according to S. Li *et al*. (2022) [18].

Measuring the levels of inflammatory cytokines gave us additional support for these findings. In animals treated with the extract-loaded chitosan nanoparticles, key markers like TNF-α, IL-1β, nitric oxide (NO), and COX-2 were significantly lower in their paw tissues. Since these molecules play a major role in driving inflammation and cancer development, their reduction adds strong evidence that the nano formulations are effectively fighting both inflammation and tumor growth. While many plant-based polyphenols and flavonoids are known to work through similar pathways, packaging them into nanoparticles helps improve their stability and how well the body can use them(Belotti *et al*., 2022; Grewal & Salar, 2024; Ismail *et al*., 2025; Liu *et al*., 2023; Ngoua-Meye-Misso *et al*., 2018; Xue *et al*., 2024; Zhao *et al*., 2021) [4, 9, 13, 19, 24, 35, 37]. The present study emphasizes the advantage of tackling cancer from two angles at once: reducing inflammation while directly encouraging tumor cells to undergo programmed cell death. This approach is especially important in colorectal cancer (CRC), where inflammation not only fuels tumor growth but also helps cancer get started in the first place. By calming the inflammatory environment and interfering with the cancer's growth signals, ID-CSNPs and JG-CSNPs offer a promising treatment strategy that fits well with the idea of multi-targeted cancer therapy attacking the disease on multiple fronts for better results.

The superiority of nano-formulated extracts over free extracts likely stems from multifaceted factors underlying their vastly differing efficacy quite evidently. Chitosan's mucoadhesive properties significantly enhance gastrointestinal absorption which is crucial for effective oral delivery of certain drugs. Nanoparticle matrix shields bioactive compounds quite effectively from degradation enabling sustained release and rather remarkably better pharmacokinetics. Fluorescence microscopy images revealed intense uniform intracellular localization mostly in CSNP-treated cells rather than cells treated with free extract. *Ipomoea digitata* tuber and *Jatropha gossypiifolia* leaf extracts used together traditionally in ethnomedicine for inflammatory diseases and cancers offer phytochemical synergy that remarkably enhances efficacy therapeutically. For instance, β-sitosterol flavonoids and terpenoids found in both plants inhibit tumor growth effectively via cell signaling pathway modulation. Stabilized within nanoparticle matrices, these compounds may exert profoundly sustained effects on various cellular pathways very effectively somehow.

Our findings in this present study collectively bolster the hypothesis that chitosan nanoparticle delivery systems enhance pharmacological properties of traditional medicinal plants effectively nowadays. From this study, the dual inhibition of Wnt/β-catenin and NF-κB two master regulators crucially involved in colorectal cancer onset provides a rational basis for developing nano formulations as adjuvant therapies in colorectal cancer (CRC) management quite effectively.

In summary, our study shows that CSNPs carrying extracts from *I. digitata* and *J. gossypiifolia* have strong anticancer effects against colorectal cancer cells. They work by triggering the cancer cells to undergo programmed cell death (apoptosis), reducing inflammation, and influencing key cancer-related signaling pathways (NF-κB, Wnt/β-catenin, and MAPK). These results highlight the exciting potential of combining modern nanotechnology with traditional medicinal plants to create new, multi-targeted treatments for complex diseases like colorectal cancer.

5. Conclusion
The present study provides compelling evidence that chitosan nanoparticles encapsulating *Ipomoea digitata* tuber and *Jatropha gossypiifolia* leaf extracts exhibit significant anticancer and anti-inflammatory properties. The nano formulations demonstrated enhanced cellular uptake, potent apoptosis induction, and strong inhibitory effects on colorectal cancer cell proliferation. This was achieved through the suppression of key oncogenic signaling pathways, namely NF-κB, Wnt/β-catenin, and MAPK, which are critically implicated in colorectal tumorigenesis. Importantly, the extract-loaded nanoparticles effectively attenuated pro-inflammatory cytokine levels and edema in animal models, affirming their therapeutic potential beyond cytotoxicity. The synergistic combination of traditional

medicinal plants and nanotechnology offers a promising strategy for the development of safe, multi-targeted interventions against colorectal cancer. These findings justify the ethnomedicinal use of *I. digitata* and *J. gossypiifolia* and underscore the role of chitosan-based nano-delivery systems in enhancing the bioavailability and efficacy of phytochemicals. Further *in vivo*, pharmacokinetic, and mechanistic studies are recommended to support clinical translation of these nano formulations as novel adjuvant therapies in colorectal cancer management. Finally, identification of specific bioactive constituents responsible for observed effects would help elucidate molecular mechanisms precisely and enable standardization of future formulations.

6. Authorship contribution statement
Cletus Anes Ukwubile: Conceptualization, Writing-original draft, Methodology, Data curation, Formal analysis, Visualization. **Aliyu Nuhu:** Methodology, Formal analysis, Data curation. **Ademola Clement Famurewa:** Methodology, Formal analysis, Literature review. **Henry Nettey:** Supervision, Formal analysis, Validation. **Jude Amakaeze Odugu:** Methodology, Formal analysis, Validation. All authors read and approval the final manuscript for submission.

7. Consent for publication
Not applicable.

8. Ethics approval
The animal study was reviewed and approved by the Animal Research Ethics Committee (AREC) of the Faculty of Pharmacy University of Maiduguri, Nigeria with approval number FP/03/24/SP.9788.

9. Declaration of Competing interest
The authors would like to affirm that they have no financial interests that could have influenced this work.

10. Acknowledgements
The authors are grateful to Mr. Jude A. Odugu of Federal Medical Center, Abuja, Nigeria for his technical assistance in some aspects of this work.

11. Abbreviations

MTT	3-(4,5-Dimethylthiazol-2-yl)-2,5- diphenyltetrazolium bromide
HCT116	Human Colorectal Carcinoma Tumor 116
SW480	Southwestern 480
COX-2	Cyclooxygenase-2
NF-kB	Nuclear Factor Kappa-Light-Chain-Enhancer of Activated B Cells
IL-1B	Interleukin-1 Beta
TNF	Tumor Necrosis Factor
ELISA	Enzyme-Linked Immunosorbent Assay
DNA	Deoxyribonucleic Acid
FITC	Fluorescein Isothiocyanate
PI	Propidium Iodide
AKT	Protein Kinase B (also known as AKT)
MAPK	Mitogen-Activated Protein Kinase
ERK1/2	Extracellular Signal-Regulated Kinase 1 and 2
MEK1/2	Mitogen-Activated Protein Kinase Kinase 1 and 2
GAPDH	Glyceraldehyde 3-Phosphate Dehydrogenase

12. Data availability
Data will be made available on request.

13. References
1. Al-Baaj AS, Abdul-Jalil TZ. Phytochemical Screening of Petroleum Ether Fractions by GC/MS and Isolation of Lupeol from Two Different Parts of Iraqi Leucaena leucocephala. Iraqi Journal of Pharmaceutical Sciences. 2022; 31(1):62-74. Doi: https://doi.org/10.31351/vol31issSuppl.pp62-74
2. Alabsi AM, Ali R, Ali AM, Al-Dubai SAR, Harun H, Kasim NHA, Alsalahi A. Apoptosis induction, cell cycle arrest and *in vitro* anticancer activity of gonothalamin in a cancer cell lines. Asian Pacific Journal of Cancer Prevention. 2012; 13(10):5131-5136. Doi: https://doi.org/10.7314/APJCP.2012.13.10.5131
3. Alam F, Din KM, Rasheed R, Sadiq A, Jan MS, Minhas AM, *et al*. Phytochemical investigation, anti-inflammatory, antipyretic and antinociceptive activities of Zanthoxylum armatum DC extracts-*in vivo* and *in vitro* experiments. Heliyon. 2020; 6(11):e05571. Doi: https://doi.org/10.1016/j.heliyon.2020.e05571
4. Belotti Y, Tolomeo S, Yu R, Lim W. With Immune Response, Inflammation and Cancer Hallmarks in Brain Tumors, 2022.
5. El Sayed AM, Basam SM, El-Naggar EM, Bellah A, Marzouk HS, El-Hawary S. LC-MS/MS and GC-MS profiling as well as the antimicrobial effect of leaves of selected Yucca species introduced to Egypt. Scientific Reports. 2020; 10(1):1-15. Doi: https://doi.org/10.1038/s41598-020-74440-y
6. Ezez D, Mekonnen N, Tefera M. Phytochemical analysis of Withania somnifera leaf extracts by GC-MS and evaluating antioxidants and antibacterial activities. International Journal of Food Properties. 2023; 26(1):581-590. Doi: https://doi.org/10.1080/10942912.2023.2173229
7. Fearon K, Strasser F, Anker SD, Bosaeus I, Bruera E, Fainsinger RL, *et al*. Definition and classification of cancer cachexia: An international consensus. The Lancet Oncology. 2011; 12(5):489-495. Doi: https://doi.org/10.1016/S1470-2045(10)70218-7
8. Félix-Silva J, Souza T, Camara RB, Arro G, Cabral B, Silva-Júnior AA, *et al*. *In vitro* anticoagulant and antioxidant activities of Jatropha gossypiifolia L. (Euphorbiaceae) leaves aiming therapeutical applications. BMC Complementary and Alternative Medicine. 2014; 14:405. Doi: https://doi.org/10.1186/1472-6882-14-405
9. Grewal AK, Salar RK. Chitosan nanoparticle delivery systems: An effective approach to enhancing efficacy and safety of anticancer drugs. Nano TransMed, May 3, 2024, 100040. Doi: https://doi.org/10.1016/j.ntm.2024.100040
10. Grivennikov SI, Greten FR, Karin M. Immunity, inflammation, and cancer. Cell. 2010; 140(6):883-899. Doi: https://doi.org/10.1016/j.cell.2010.01.025.Immunity
11. Guo J, Liu Y. INHBA promotes the proliferation, migration and invasion of colon cancer cells through the upregulation of VCAN. Journal of International Medical Research. 2021; 49(6). Doi: https://doi.org/10.1177/03000605211014998

12. Herdiana Y, Wathoni N, Shamsuddin S, Muchtaridi M. Drug release study of the chitosan-based nanoparticles. Heliyon. 2022; 8(1):e08674. Doi: https://doi.org/10.1016/j.heliyon.2021.e08674

13. Ismail KM, Hassan SS, Hanna DH. Palladium-Imidazole Nanoparticles' Cytotoxic Effects on Colon Cancer Cells: Induction of Cell Cycle Arrest and Apoptosis Mediated via Mitochondria. Applied Organometallic Chemistry. 2025; 39(1):e7908. Doi: https://doi.org/https://doi.org/10.1002/aoc.7908

14. Javid A, Ahmadian S, Saboury AA, Kalantar SM, Rezaei-Zarchi S. Chitosan-coated superparamagnetic iron oxide nanoparticles for doxorubicin delivery: Synthesis and anticancer effect against human ovarian cancer cells. Chemical Biology and Drug Design. 2013; 82(3):296-306. Doi: https://doi.org/10.1111/cbdd.12145

15. Kandilarov I, Gardjeva P, Georgieva-Kotetarova M, Zlatanova H, Vilmosh N, Kostadinova I, et al. Effect of Plant Extracts Combinations on TNF-α, IL-6 and IL-10 Levels in Serum of Rats Exposed to Acute and Chronic Stress. Plants. 2023; 12(17):2-17. Doi: https://doi.org/10.3390/plants12173049

16. Letaief T, Garzoli S, Laghezza Masci V, Mejri J, Abderrabba M, Tiezzi A, et al. Chemical composition and biological activities of tunisian ziziphus lotus extracts: Evaluation of drying effect, solvent extraction, and extracted plant parts. Plants. 2021; 10(12). Doi: https://doi.org/10.3390/plants10122651

17. Li J, Cai C, Li J, Li J, Li J, Sun T, et al. Chitosan-based nanomaterials for drug delivery. Molecules. 2018; 23(10):1-26. Doi: https://doi.org/10.3390/molecules23102661

18. Li S, Zhang H, Chen K, Jin M, Vu SH, Jung S, et al. Application of chitosan/alginate nanoparticle in oral drug delivery systems: Prospects and challenges. Drug Delivery. 2022; 29(1):1142-1149. Doi: https://doi.org/10.1080/10717544.2022.2058646

19. Liu X, Yin L, Shen S, Hou Y. Inflammation and cancer: Paradoxical roles in tumorigenesis and implications in immunotherapies. Genes and Diseases. 2023; 10(1):151-164. Doi: https://doi.org/10.1016/j.gendis.2021.09.006

20. Lukiati B, Sulisetijono Nugrahaningsih, Masita R. Determination of total phenol and flavonoid levels and antioxidant activity of methanolic and ethanolic extract zingiber officinale rosc var. rubrum rhizome. AIP Conference Proceedings, 2020, 2231. Doi: https://doi.org/10.1063/5.0002657

21. Madan NV, Karole S. In vitro Cytotoxicity studies on Ipomoea digit at a -An important Traditional Medicinal Plant. 2022; 20(20):3023-3029. Doi: https://doi.org/10.48047/NQ.2022.20.20.NQ109299

22. Malviya S, Malviya N, Joshi A, Johariya V, Saxena R. Medicinal Plants and Cancer Chemoprevention. Medicinal Plants and Cancer Chemoprevention. 2023; 9(7):1-232. Doi: https://doi.org/10.1201/9781003251712

23. Maraicar KSH, Narayanan T. Design and Characterization of Solid Lipid Nanoparticle by Solvent Evaporation Method Followed by Homogenization. International Journal of Biopharmaceutics. 2014; 5(3):190-196.

24. Ngoua-Meye-Misso R-L, Ndong JDLC, Sima-Obiang C, Ondo JP, Ndong-Atome GR, Ovono Abessolo F, et al. Correction to: Phytochemical studies, antiangiogenic, antiinflammatory and antioxidant activities of Scyphocephalium ochocoa Warb. (Myristicaceae), medicinal plant from Gabon. Clinical Phytoscience. 2018; 4(1). Doi: https://doi.org/10.1186/s40816-018-0078-7

25. Oppong MB, Cao S, Fang SM, Amponsah SK, Donkor PO, Lartey M, et al. In-vitro and in-vivo anti-inflammatory properties of extracts and isolates of Pangdahai. Phytomedicine Plus. 2024; 4(2):100533. Doi: https://doi.org/10.1016/j.phyplu.2024.100533

26. Paramee S, Sookkhee S, Sakonwasun C, Na Takuathung M, Mungkornasawakul P, Nimlamool W, et al. Anti-cancer effects of Kaempferia parviflora on ovarian cancer SKOV3 cells. BMC Complementary and Alternative Medicine. 2018; 18(1):1-13. Doi: https://doi.org/10.1186/s12906-018-2241-6

27. Raval J, Patel J, Patel M. Formulation and in vitro characterization of spray dried microspheres of amoxicillin. Acta Pharmaceutica. 2010; 60(4):455-465. Doi: https://doi.org/10.2478/v10007-010-0034-7

28. Shah MS, Tayab MA, Rahman A, Hasan MN, Talukder MSH, Uddin AMK, et al. Anxiolytic, antidepressant and antioxidant activity of the methanol extract of Canarium resiniferum leaves. Journal of Traditional and Complementary Medicine. 2022; 12(6):567-574. Doi: https://doi.org/10.1016/j.jtcme.2022.07.001

29. Sultan MH, Moni SS, Madkhali OA, Bakkari MA, Alshahrani S, Alqahtani SS, et al. Characterization of cisplatin-loaded chitosan nanoparticles and rituximab-linked surfaces as target-specific injectable nano-formulations for combating cancer. Scientific Reports. 2022; 12(1):1-16. Doi: https://doi.org/10.1038/s41598-021-04427-w

30. Sung H, Ferlay J, Siegel RL, Laversanne M, Soerjomataram I, Jemal A, et al. Global Cancer Statistics 2020: GLOBOCAN Estimates of Incidence and Mortality Worldwide for 36 Cancers in 185 Countries. CA: A Cancer Journal for Clinicians. 2021; 71(3):209-249. Doi: https://doi.org/10.3322/caac.21660

31. Ukwubile CA. Phytochemical Content and Anti-Inflammatory Potential of Solanum americanum Mill. (Solanaceae) Methanol Leaf Extract in Wistar Rats. International Journal of Complementary and Internal Medicine, 2024. Doi: https://doi.org/10.58349/IJCIM.1.6.2024.00140

32. Ukwubile CA, Malgwi TS, Nuhu A, Menkiti ND. Toxicity, cytotoxicity, and anti-inflammatory activities of polyphenols from Guiera senegalensis J. F. Gmel. Leaf extract. Journal of Ethnopharmacology and Toxicology. 2025; 3(1):1-22. Doi: 10.37446/jet/rsa/3.1.2025.1-22

33. Van Der Willik KD, Koppelmans V, Hauptmann M, Compter A, Ikram MA, Schagen SB. Inflammation markers and cognitive performance in breast cancer survivors 20 years after completion of chemotherapy: A cohort study. Breast Cancer Research. 2018; 20(1):1-10. Doi: https://doi.org/10.1186/s13058-018-1062-3

34. Wei W, Guo Q, Guo C, Cui X, Ma X, Shen X, et al. Ginsenoside Rh2 Suppresses Metastasis and Growth of Colon Cancer via miR-491. Journal of Oncology, 2021. Doi: https://doi.org/10.1155/2021/6815713

35. Xue Y, Ruan Y, Wang Y, Xiao P, Xu J. Signaling pathways in liver cancer: Pathogenesis and targeted

therapy. Molecular Biomedicine. 2024; 5(1). Doi: https://doi.org/10.1186/s43556-024-00184-0

36. Younes I, Rinaudo M. Chitin and chitosan preparation from marine sources. Structure, properties and applications. Marine Drugs. 2015; 13(3):1133-1174. Doi: https://doi.org/10.3390/md13031133

37. Zhao H, Wu L, Yan G, Chen Y, Zhou M, Wu Y, *et al*. Inflammation and tumor progression: signaling pathways and targeted intervention. Signal Transduction and Targeted Therapy. 2021; 6(1). Doi: https://doi.org/10.1038/s41392-021-00658-5